

# Edge critical behavior at the surface transition of Ising magnets

M. Pleimling and W. Selke

*Institut für Theoretische Physik B, Technische Hochschule, D-52056 Aachen, Germany*

Using Monte Carlo techniques, Ising models with ferromagnetic nearest-neighbor interactions on a simple cubic lattice are studied. At the surface transition, the critical exponent  $\beta_2$  of the edge magnetization is found to be non-universal, depending on the edge and edge-surface couplings, in contrast to the situation at the ordinary transition. Results are compared to those for two-dimensional Ising magnets with chain and ladder defects.

*Pacs numbers:* 05.50+q, 68.35.Rh, 75.40.Mg

## I. Introduction

Critical phenomena occur not only in the bulk of a system, but also at its surfaces and edges. To be specific, let us consider the magnetization as the order parameter. Then, there are two typical scenarios: (a) bulk,  $m_b$ , surface,  $m_1$ , and edge,  $m_2$ , magnetizations may order at the same temperature ('ordinary transition'), but with different power-laws, and (b) surface and edge may order first ('surface transition') due to strong surface couplings, followed by ordering of the bulk magnetization ('extraordinary transition') at a lower temperature. Surface singularities at ordinary and surface transitions have been studied extensively for various systems, theoretically<sup>1,2</sup> as well as experimentally.<sup>3</sup> Edge critical behavior, on the other hand, has attracted less attention.

Some years ago, Cardy noted and calculated the dependence of edge critical exponents on the opening angle between the surfaces forming the edge, using mean field theory and renormalization group theory of first order in  $\epsilon$  for  $O(n)$  models at the ordinary transition.<sup>4</sup> Subsequent work dealt mainly with edge criticality at the ordinary transition as well, including high temperature series expansions<sup>5</sup>, exact analyses of two-dimensional Ising models<sup>6</sup>, and applications to polymers.<sup>7</sup>

In recent Monte Carlo simulations of three-dimensional Ising models, we confirmed and refined the estimates obtained from renormalization group calculations and high temperature series expansions on edge critical exponents at the ordinary transition, especially on  $\beta_2$  describing the vanishing of the edge magnetization  $m_2$  on approach to criticality.<sup>8</sup> The value of  $\beta_2$  varies with the opening angle, but not with the bulk, surface and edge coupling constants which are assumed to be ferromagnetic and of short range.

Edge critical properties at the surface transition have been largely overlooked. Actually, we are aware of merely one exception, where they have been mentioned briefly and qualitatively.<sup>9</sup> However, that case deserves to be in-

vestigated, in particular, by Monte Carlo techniques in the framework of Ising models, too. At the surface transition in three-dimensional systems, the critical fluctuations are essentially two-dimensional, and the surface critical exponents reflect the reduced dimensionality.<sup>1,2</sup> On the other hand, the edge presents a local perturbation, acting presumably like the much studied chain or ladder defects<sup>10–14</sup> in two-dimensional Ising systems. Following those studies, intriguing non-universal edge critical behavior, depending on the interactions at the edge, may be expected, in contrast to the situation at the ordinary transition. Furthermore, previous Monte Carlo simulations on the critical properties of Ising models at surfaces, edges, and corners<sup>8,15–17</sup> show that present simulational techniques, especially cluster-flip algorithms, allow to estimate reliably edge critical properties. Accordingly, the simulational results may provide guidance for future analytical investigations. Finally, the findings may encourage experimental search for suitable magnets or alloys<sup>3</sup>, where the surface coupling is sufficiently strongly enhanced compared to the bulk coupling.

The outline of the article is as follows. In the next section, the model and its phase diagram as well as the Monte Carlo method will be introduced. In section 3, we shall discuss magnetization profiles and the critical exponent of the edge magnetization at the surface transition in the three-dimensional Ising model for various couplings near the edges. A brief summary concludes the paper.

## II. Ising model with surfaces and edges

We study nearest-neighbor Ising models on simple cubic lattices with ferromagnetic interactions. The Hamiltonian may be written in the form

$$\mathcal{H} = - \sum_{\text{bulk}} J_b S_{xyz} S_{x'y'z'} - \sum_{\text{surface}} J_s S_{xyz} S_{x'y'z'} - \sum_{\text{edge-surface}} J_{es} S_{xyz} S_{x'y'z'} - \sum_{\text{edge}} J_e S_{xyz} S_{x'y'z'} \quad (1)$$

where the sums run over bonds between neighboring spins,  $S_{xyz} = \pm 1$ , with coupling constants to be specified below. Free boundary conditions hold for the spins in the  $yz$ - and  $xz$ -surface planes, while the spins in the first and last  $xy$ -planes are connected by periodic boundary conditions, see Fig.1. Thereby the edges formed by the intersecting free surface planes are oriented along the  $z$ -axis. The total number of sites or spins is  $L \times M \times N$ , where  $L$ ,  $M$ , and  $N$  correspond to the  $x$ ,  $y$ , and  $z$ -directions, respectively. In the following, we assume  $L = M$ , i.e. there are  $L^2$  spins in each plane perpendicular to the edges. The pairs of spins in the Hamiltonian (1) are situated

either on edges with the edge coupling  $J_e$ , on edge and surface sites coupled by  $J_{es}$ , on surface sites with the interaction  $J_s$ , or with at least one of the spins in the interior of the system interacting with the bulk coupling  $J_b$ , as depicted in Fig. 1.

The magnetization per site for lines parallel to the  $z$ -axis,  $m_l(x, y)$ , is defined as

$$m_l(x, y) = \langle |\sum_z S_{xyz}| \rangle / N \quad (2)$$

summing over all spins of a line, with  $x$  and  $y$  being fixed. The brackets denote thermal averages. The absolute value is taken to avoid vanishing magnetizations for finite systems, as usual. The edge magnetization,  $m_2$ , is then identical to  $m_l(1, 1) = m_l(1, L) = m_l(L, 1) = m_l(L, L)$ . The surface magnetization,  $m_1$ , is given by  $m_l(1, L_C) = m_l(L_C, L) = m_l(L_C, 1) = m_l(L, L_C)$ , where  $L_C$  refers to the one or two center lines, with  $L_C = (L + 1)/2$  or  $L_C = L/2 \pm 1$ . The profile of the line magnetization at the surface,  $m_{ls}(i)$ , is described by

$$m_{ls}(i) = (m_l(x, L) + m_l(x, 1) + m_l(1, y) + m_l(L, y)) / 4 \quad (3)$$

with, setting the lattice constant equal to one,  $i = x = y = 1, 2, \dots, L$  (certainly, the profile is symmetric around  $i = L_C$ ). The bulk magnetization,  $m_b$ , corresponds to  $m_l(L_C, L_C)$ .

Of course, the line magnetizations may be affected by finite size effects. The thermodynamic limit is approached when  $L, M, N \rightarrow \infty$ .

To elucidate bulk, surface, and edge properties of the model, we considered a few additional quantities. In particular, we calculated the energy of the surface spins,  $E_s$ , the energy of the edge spins,  $E_e$ , the edge susceptibility  $\chi_{22}$  (defined as the fluctuation of the edge magnetization<sup>4</sup>), and higher moments of various magnetizations (Binder cumulants).

The linear dimensions,  $L$  and  $N$ , of the  $L^2 \times N$  systems ranged from  $L = 10$  to  $L = 80$ , and from  $N = 10$  to  $N = 160$ . We used the efficient one-cluster-flip Monte Carlo algorithm, which reduces significantly critical slowing down. Typically, averages were taken over a few  $10^4$  clusters, after equilibration. Error bars resulted from sampling over several realizations.

The phase diagram of the Ising model (1) is determined by the ratio of the surface to the bulk coupling,  $r = J_s/J_b$ ,<sup>1,2,16–18</sup> see Fig. 2. At  $r < r_c \approx 1.50$ , the model displays an ordinary transition, with bulk,  $m_b$ , and surface magnetizations,  $m_1$ , ordering simultaneously at the bulk transition temperature,  $T_c = 4.5115\dots J/k_B$ .<sup>19,20</sup> The surface critical exponents are universal, i.e. independent of the ratio  $r$ . For instance, the surface magnetization  $m_1$  vanishes on approach to  $T_c$  as  $m_1 \propto t^{\beta_1}$ , where  $t = |T - T_c|/T_c$  is the reduced temperature, with  $\beta_1 = 0.80 \pm 0.01$ <sup>17</sup> (this value is robust against randomness in the surface couplings and corrugations of the

surface<sup>17,21</sup>). At  $r = r_c \approx 1.50$ , bulk and surface still order at the same temperature,  $T_c$ , but the surface critical exponents at this 'special point' are in a different universality class, e.g.,  $\beta_1 \approx 0.24$ .<sup>1,2</sup>

At  $J_s > r_c J_b$ , the surface magnetization  $m_1$  orders at the surface transition, with the critical temperature  $T_s$  being higher than that of the bulk ordering which occurs at the extraordinary transition,  $T_c$ . At  $T_s$ , the surface critical fluctuations are of two-dimensional character, and the surface critical exponents are those of the two-dimensional Ising model with nearest-neighbor interactions<sup>1,2</sup>, i.e., for example,  $\beta_1 = 1/8$ .

Because edges are one-dimensional, and all couplings in the models are of short range, one expects edge quantities to become singular at the surface transition,  $T_s$ , but the edge critical exponents may differ from the corresponding surface values<sup>8</sup> (similar to the critical behavior at one-dimensional surfaces in two-dimensional Ising models<sup>22</sup>). Most of the Monte Carlo simulations near  $T_s$  were done at fixed ratio  $r = J_s/J_b = 2$ , varying then the nearest neighbor interactions along the edges,  $J_e$ , and between edge and surface spins,  $J_{es}$ , with  $J_e$  ranging from 0 to  $2J_s$ , and  $J_{es}$  ranging from  $0.5J_s$  to  $2J_s$ .

To determine edge critical exponents accurately,  $T_s$  needs to be determined accurately. Using standard finite-size analyses<sup>23</sup> (with the scaling variable  $Nt$ , implying that the surface fluctuations are governed by the surface correlation length which diverges like  $t^{-1}$ ),  $T_s$  may be obtained from the location of turning points or extrema in various thermal quantities. As illustrated and indicated in Fig. 3, different quantities give, indeed, consistent estimates. For  $r = 2$ , we find  $T_s = 4.9575 \pm 0.0075$ . Note that other critical temperatures of the surface transition, needed to map the phase diagram, Fig. 2, have been obtained with less accuracy, by doing finite-size analyses on the location of the turning point of the surface magnetization for systems of moderate sizes, with up to  $40^3$  sites.

### III. Magnetization profiles and edge critical exponents

The profiles of the line magnetization at the surface,  $m_{ls}(i)$ , equation (3), reflect the influence of bulk spins close to the surfaces and edges as well as the strength of the couplings near the edges,  $J_e$  and  $J_{es}$ .

Typical profiles are shown in Fig. 4. At  $J_e = J_{es} = J_s (= 2J_b)$ , i.e., for equal edge, edge-surface, and surface couplings, the effect of the bulk spins near the surfaces and edges on the temperature dependence of the profile is illustrated in Fig. 4a. At low temperatures,  $m_{ls}(i)$  increases monotonically with  $i$ , i.e. the distance from the edge. The magnetization of the surface spins, which are connected directly to an ordered bulk spin, is enhanced compared to the edge magnetization,  $m_2 = m_{ls}(1)$ . Edge spins have the coordination number four, while it is five for the surface spins. In contrast, on approach to  $T_s$ , the ordering of the spins falls off quickly by going from the surface to the bulk, and the surface magnetization,

$m_1 = m_{ls}(L_C)$ , is pulled down below the edge magnetization by the coupling to the bulk spin. Roughly at temperatures above  $T_c$ , an interesting non-monotonic behavior in the profile shows up, with a maximum close to the edge. It may be explained by the fact that surface spins next to, but on different sides of an edge, are more strongly connected to each other, through the same neighboring bulk spin, than spins on the flat part of the surface with the separation distance of two.

The profile approaches the surface magnetization  $m_1$  nearly exponentially already at rather small distances from the maximum, i.e.  $|m_{ls}(i) - m_1| \propto \exp(-ai)$ ;  $a$  is expected to be, as  $T \rightarrow T_s$ , the inverse correlation length.<sup>1,2,8</sup>

In Fig. 4b, the influence of the edge and edge-surface couplings,  $J_e$  and  $J_{es}$ , on the profile, at fixed temperature, is illustrated. The trends may be readily understood. By increasing the coupling,  $J_e$ , along an edge, the edge magnetization will rise. Likewise, a larger interaction,  $J_{es}$ , of the edge spins with the neighboring surface spins will lead to an increase of the edge magnetization. In that case, the non-monotonic shape of the profile close to the edge sets in at lower temperatures.

Near the surface transition, where the critical fluctuations are of two-dimensional character, the edge acts like a defect line in an essentially two-dimensional bulk Ising model;  $J_e$  corresponds to a 'chain defect' and  $J_{es}$  to a 'ladder-type defect'.<sup>14</sup> The change in the topology at the edge compared to the surface amounts to a complicated ladder-type defect.

This analogy will be crucial in explaining the simulational findings on the critical exponent  $\beta_2$  of the edge magnetization, defined by

$$m_2 \propto t^{\beta_2} \quad (4)$$

where  $t$  is the reduced temperature of the surface transition,  $t = |T_s - T|/T_s$ ,  $t \rightarrow 0$ . To estimate  $\beta_2$ , we consider the effective exponent<sup>8,17</sup>

$$\beta_{eff} = d \ln m_2 / d \ln t \quad (5)$$

In analysing Monte Carlo data, the derivative is replaced by a difference at discrete temperatures.  $\beta_{eff}$  approaches  $\beta_2$  as  $t \rightarrow 0$ , provided finite-size effects can be neglected.

To check whether the edge magnetization  $m_2$  is affected by the finite size of the Monte Carlo system, one may proceed as follows. First, one chooses, at fixed temperature, the linear dimensions  $L$  and  $N$  to be sufficiently large to reproduce the numerically to a high degree of accuracy known thermodynamic bulk,  $m_b = m_l(L_C, L_C)$ , and surface,  $m_1 = m_{ls}(L_C)$ , magnetizations. In a second step,  $N$  may be enlarged to search for further size dependences in  $m_2$ .<sup>8</sup>

In Fig. 5, the effective exponent  $\beta_{eff}$  of the edge magnetization is displayed for various system sizes, in the case of equal surface and edge couplings  $J_e = J_{es} = J_s = 2J_b$ .

Obviously,  $\beta_{eff}$  increases on lowering the reduced temperature before it acquires, at  $t < 0.15$ , nearly a plateau. Finally, on further approach to  $T_s$ , it decreases to zero due to a non-vanishing edge magnetization at the critical point in finite systems. Monte Carlo data which are largely free of finite-size dependences have been obtained down to  $t \approx 0.06$ , using systems with up to  $80^3$  spins. Assuming the plateau-like behavior,  $0.06 < t < 0.15$ , to hold even closer to  $T_s$  (which would imply that corrections to scaling, i.e. to the asymptotic power-law, equation (4), are small), we arrive at the estimate of the critical exponent  $\beta_2$  for this set of coupling constants,  $\beta_2 = 0.095 \pm 0.005$ . Error bars in Fig. 5 include both sample averaging and the uncertainty in  $T_s$ , see above. Here and in the following, the error bar for the value of  $\beta_2$  is rather subjective, based on 'reasonable' extrapolation of the data, which are close to those in the thermodynamic limit, to  $t \rightarrow 0$ .

The critical exponent  $\beta_2$  is significantly lower than the critical exponent of the surface magnetization,  $\beta_1 = 1/8$ , reflecting the fact that the edge magnetization is, on approach to  $T_s$ , larger than the surface magnetization. We may relate this finding to results for two-dimensional nearest-neighbor Ising model with a ladder defect. In that model, the couplings are identical, say,  $J > 0$ , throughout the system with the exception of the couplings,  $J_l$ , of the spins in one row to the spins in a neighboring row. The ladder rows correspond to the edge, and the ladder couplings,  $J_l$ , reflect not only the edge-surface interactions  $J_{es}$ , but also the change in topology (or connectedness to bulk spins) at the edge compared to the surface. For the two-dimensional Ising model with a ladder defect, the critical exponent  $\beta_l$  of the magnetization in the ladder rows has been determined exactly<sup>11,12</sup>,

$$\beta_l = 2 \arctan^2(\kappa_l^{-1})/\pi^2 \quad (6)$$

with  $\kappa_l = \tanh(J_l/(k_B T_{2d})) / \tanh(J/(k_B T_{2d}))$ , where  $T_{2d}$  is the transition temperature. Thence, the critical exponent of the ladder row magnetization varies monotonically with the strength of the coupling  $J_l$ , being smaller than  $1/8$  when  $J_l > J$ . Comparing the critical exponents  $\beta_l$  and  $\beta_2$ , one may attribute an effective ladder coupling  $J_l$  to the edge. Our case,  $J_e = J_{es} = J_s = (2J_b)$ , corresponds to  $J_l > J (= J_s)$ . Of course, the non-monotonic profiles of the line magnetization suggest that a closer analogy between edge properties and descriptions by two-dimensional Ising models with defect lines would require more complicated, extended ladder-type defects, which have not been treated analytically so far.<sup>14</sup>

At any rate, exact results on two-dimensional Ising models with defect lines of different types<sup>14,11,12</sup> provide a useful framework to discuss our simulational findings on the dependence of  $\beta_2$  on the edge and edge-surface couplings,  $J_e$  and  $J_{es}$ . Obviously,  $J_{es}$  is intimately related to  $J_l$ , while changing  $J_e$  may be interpreted as modifying nearest-neighbor couplings,  $J_{ch}$ , along a single defect line or chain in the two-dimensional Ising model. For a chain

defect, the critical exponent,  $\beta_{ch}$ , of the magnetization in the defect chain varies continuously as<sup>11,12</sup>

$$\beta_{ch} = 2 \arctan^2(\kappa_{ch})/\pi^2 \quad (7)$$

with  $\kappa_{ch} = \exp[-2(J_{ch}/(k_B T_{2d}) - J/(k_B T_{2d}))]$ . Again, the critical exponent changes monotonically, being larger than  $1/8$  when  $J_{ch} < J$ .

Pertinent results on the edge critical exponent  $\beta_2$  are shown in Figs. 6 and 7. In Fig. 6, the effect of weakening the interactions between the edge and the surface,  $J_{es}$ , is demonstrated. As expected from equation (6), lowering that coupling leads to an increase in the value of  $\beta_2$ . Only Monte Carlo data are depicted which seem to be unaffected by finite-size dependences, simulating systems with up to  $80^3$  sites. As before, the effective exponent  $\beta_{eff}$  exhibits a broad plateau in  $t$ , which may allow one to extrapolate the asymptotic exponent quite accurately. Our estimates, for  $J_e = J_s = 2J_b$ , are  $\beta_2 = 0.176 \pm 0.005$  at  $J_{es} = J_e/2$  and  $\beta_2 = 0.244 \pm 0.005$  at  $J_{es} = J_e/4$ .

Similarly, weakening of the edge interaction  $J_e$  tends to increase the critical exponent of the edge magnetization, see equation (7). In Fig. 7, the effective exponent  $\beta_{eff}$  is shown, using again only those simulational data for the edge magnetization which approximate closely the infinite system. In this case, the effective exponent depends on approach to  $T_s$  nearly linearly on the reduced temperature  $t$ , signalling rather strong corrections to scaling for  $m_2$ . By extrapolating the findings for  $\beta_{eff}$  to the critical point,  $t \rightarrow 0$ , we estimate, for  $J_{es} = J_s = 2J_b$ ,  $\beta_2 = 0.170 \pm 0.005$  in the limiting case  $J_e = 0$ , and  $\beta_2 = 0.127 \pm 0.005$  for  $J_e = J_{es}/2$ . The close agreement with the value of the surface critical exponent  $\beta_1 = 1/8$ , in the latter case, is rather fortuitous, due to a compensation of a reduction in  $\beta_2$  following from the increase in the effective ladder coupling stemming from the edge topology (as discussed above), and of an enhancement in  $\beta_2$  following from the decrease in the strength of the chain coupling.

The non-universality character of the edge transition driven by the surface transition is also confirmed by our findings for the critical properties of the edge susceptibility  $\chi_{22}$ . However, because the estimates are quite rough, we refrain from quoting specific values.

The Binder cumulant at  $T_s$  for the edge magnetization depends on the edge and edge-surface couplings as well. However, this may not be interpreted as additional evidence for non-universality, because that cumulant changes with, e.g., the ratio of the surface to bulk interactions  $r = J_s/J_b$  even at the ordinary transition, while the critical exponents are universal there.<sup>15</sup>

#### IV. Summary

We studied magnetization profiles and the critical exponent  $\beta_2$  of the edge magnetization of three-dimensional nearest-neighbor Ising models near the surface transition,  $T_s$  (with the surface coupling  $J_s$  being twice as large as the bulk coupling). We did large-scale simu-

lations, using the single-cluster-flip Monte Carlo algorithm. In particular, the influence of the edge,  $J_e$ , and edge-surface,  $J_{es}$ , couplings has been investigated.

The profiles of the line magnetization at the surface suggest that the edge acts like a rather complicated, extended ladder-type defect in an essentially two-dimensional Ising magnet. The reduced dimensionality is due to the two-dimensional character of the critical fluctuations at the surface transition.

The edge critical exponent  $\beta_2$  varies continuously with  $J_e$  and  $J_{es}$ . If  $J_e$  and  $J_{es}$  are equal to the surface coupling,  $\beta_2 (=0.095 \pm 0.005)$  is significantly lower than the critical exponent of the surface magnetization,  $\beta_1 = 1/8$ . When weakening the couplings at the edge,  $\beta_2$  increases monotonically. Eventually,  $\beta_2$  will be clearly larger than  $1/8$ , in accordance with related exact results for two-dimensional Ising models with defect lines. The decrease of  $J_{es}$  has a more pronounced impact on  $\beta_2$ ; the value of the edge critical exponent may exceed appreciably the limiting value obtained at vanishing  $J_e$ . By weakening  $J_e$ , strong corrections to scaling for the edge magnetization are observed.

It may be of interest to check the present Monte Carlo results by applying other methods, such as renormalization group techniques. Likewise, it may be feasible to mimic the edge by a realistic ladder-type defect in a, possibly, exactly solvable two-dimensional Ising model. Finally, the non-universality of the critical behavior is expected to show up in additional dependences of the critical exponents on details of, for instance, the lattice structure and the range of interactions.

#### Acknowledgement

We thank F. Iglói for a useful discussion.

---

<sup>1</sup> K. Binder, in *Phase Transitions and Critical Phenomena*, edited by C. Domb and J. L. Lebowitz (Academic, London, 1983), Vol. 8.

<sup>2</sup> H. W. Diehl, in *Phase Transitions and Critical Phenomena*, edited by C. Domb and J. L. Lebowitz (Academic, London, 1986), Vol. 10; H. W. Diehl, Int. J. Mod. Phys. B **11**, 3503 (1997).

<sup>3</sup> H. Dosch, *Critical Phenomena at Surfaces and Interfaces* (Springer, Berlin, Heidelberg, New York, 1992).

<sup>4</sup> J. Cardy, J. Phys. A: Math. Gen. **16**, 3617 (1983).

<sup>5</sup> A. J. Guttmann and G. M. Torrie, J. Phys. A: Math. Gen. **17**, 3539 (1984).

<sup>6</sup> M. N. Barber, I. Peschel, and P. A. Pearce, J. Stat. Phys. **37**, 497 (1984); I. Peschel, Phys. Lett. **110A**, 313 (1985); B. Davies and I. Peschel, Ann. Physik **6**, 187 (1997).

<sup>7</sup> K. de Bell and T. Lookman, Rev. Mod. Phys. **65**, 87 (1993).

<sup>8</sup> M. Pleimling and W. Selke, Eur. Phys. J. B (in print).

<sup>9</sup> T. A. Larsson, J. Phys. A: Math. Gen. **19**, 1691 (1986).

- <sup>10</sup> M. E. Fisher and A. E. Ferdinand, Phys. Rev. Lett. **19**, 169 (1967).  
<sup>11</sup> R. Z. Bariev, Sov. Phys. JETP **50**, 613 (1979).  
<sup>12</sup> B. M. McCoy and J. H. H. Perk, Phys. Rev. Lett. **44**, 840 (1980).  
<sup>13</sup> L.-F. Ko, H. Au-Yang, and J. H. H. Perk, Phys. Rev. Lett. **54**, 1091 (1985).  
<sup>14</sup> F. Iglói, I. Peschel, and L. Turban, Adv. Phys. **42**, 683 (1993).  
<sup>15</sup> D. P. Landau and K. Binder, Phys. Rev. **B 41**, 4633 (1990).  
<sup>16</sup> C. Ruge, S. Dunkelmann, and F. Wagner, Phys. Rev. Lett. **69**, 2465 (1992); C. Ruge and F. Wagner, Phys. Rev. **B 52**, 4209 (1995).  
<sup>17</sup> M. Pleimling and W. Selke, Eur. Phys. J. B **1**, 385 (1998).  
<sup>18</sup> F. Zhang, S. Thevuthasan, R. T. Scalettar, R. R. P. Singh, and C. S. Fadley, Phys. Rev. **B 51**, 12468 (1995).  
<sup>19</sup> A. M. Ferrenberg and D. P. Landau, Phys. Rev. **B 44**, 5081 (1991).  
<sup>20</sup> A. L. Talapov and H. W. J. Blöte, J. Phys. A: Math. Gen. **29**, 5727 (1996).  
<sup>21</sup> H. W. Diehl, Eur. Phys. J. B **1**, 401 (1998).  
<sup>22</sup> W. Selke, F. Szalma, P. Lajko, and F. Iglói, J. Stat. Phys. **89**, 1079 (1997).  
<sup>23</sup> M. N. Barber, in *Phase Transitions and Critical Phenomena*, edited by C. Domb and J. L. Lebowitz (Academic, London, 1983), Vol. 8; M. E. Fisher, in *Critical Phenomena*, Proc. 51st Enrico Fermi Summer School, edited by M. S. Green (Academic Press, New York, 1970).

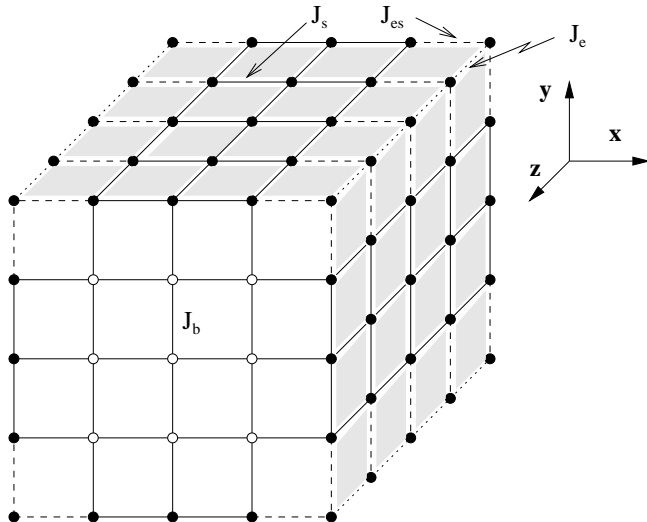


FIG. 1. Sketch of the lattice structure and the coupling constants at the edges,  $J_e$  and  $J_{es}$ , at the surface,  $J_s$ , and in the bulk,  $J_b$ .

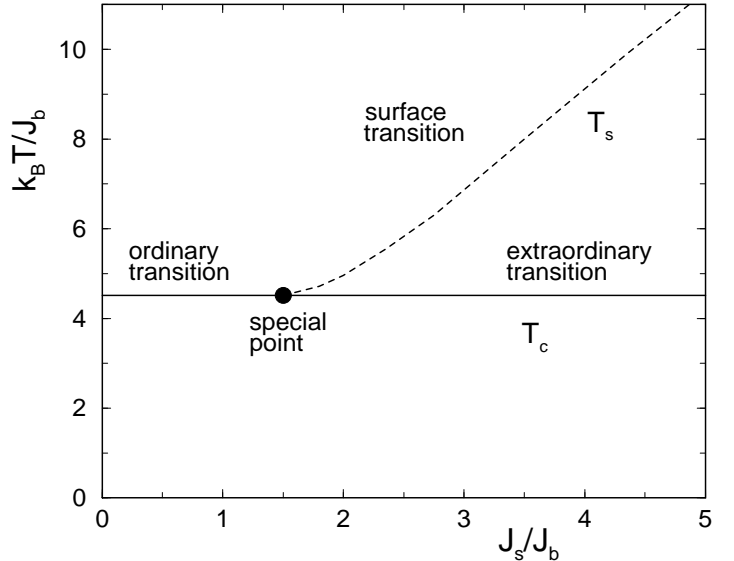


FIG. 2. Phase diagram of the three-dimensional Ising model, in the  $(k_B T / J_b, J_s / J_b)$ -plane. The dashed curve denotes the surface transition line,  $T_s$ .

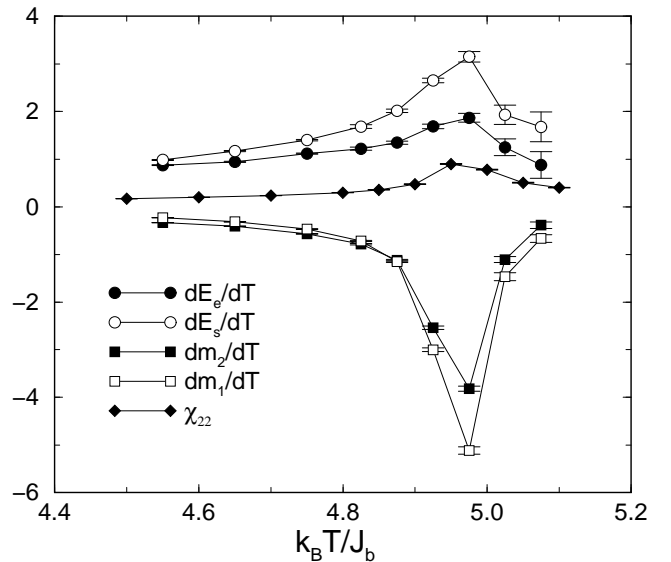


FIG. 3. Monte Carlo data on temperature dependence of the edge susceptibility,  $\chi_{22}$ , and of the temperature derivatives of the edge energy,  $E_e$ , surface energy,  $E_s$ , surface magnetization,  $m_1$ , as well as edge magnetization,  $m_2$ , near  $T_s$ , at  $J_e = J_{es} = J_s = 2J_b$  for a system of size  $40^2 \times 160$ .

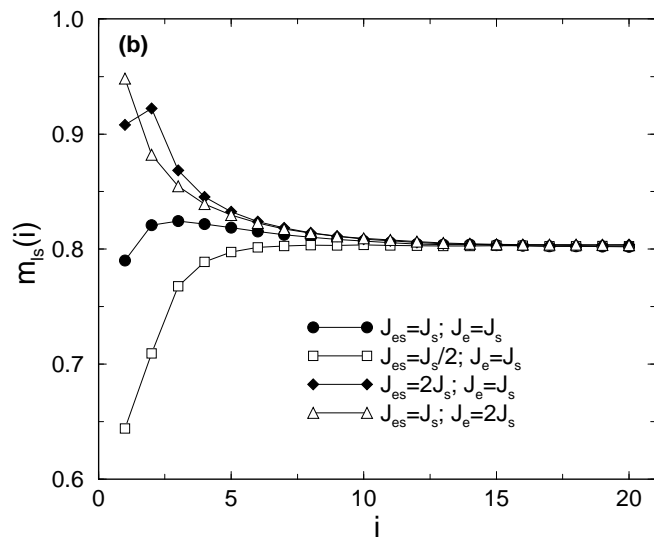
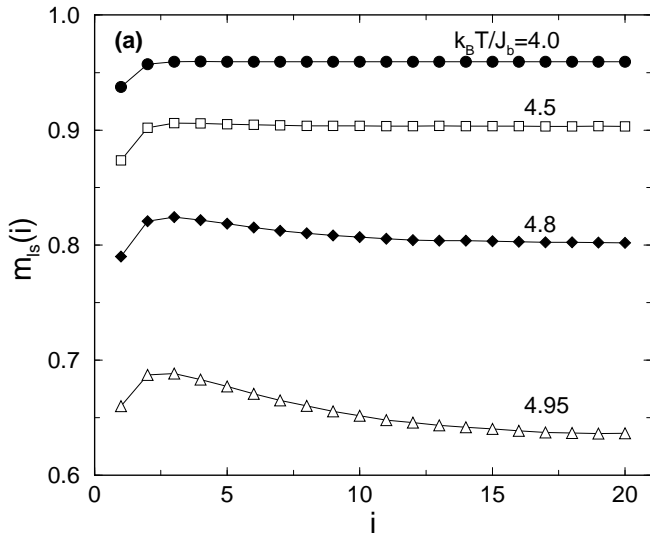


FIG. 4. Profiles of the line magnetization  $m_{ls}(i)$  at (a)  $J_e = J_{es} = J_s = 2J_b$ , with various temperatures, and (b) at fixed temperature,  $k_BT/J_b = 4.8$ , with various edge and edge-surface couplings ( $J_s = 2J_b$ ). Ising models of size  $40^3$  have been simulated.

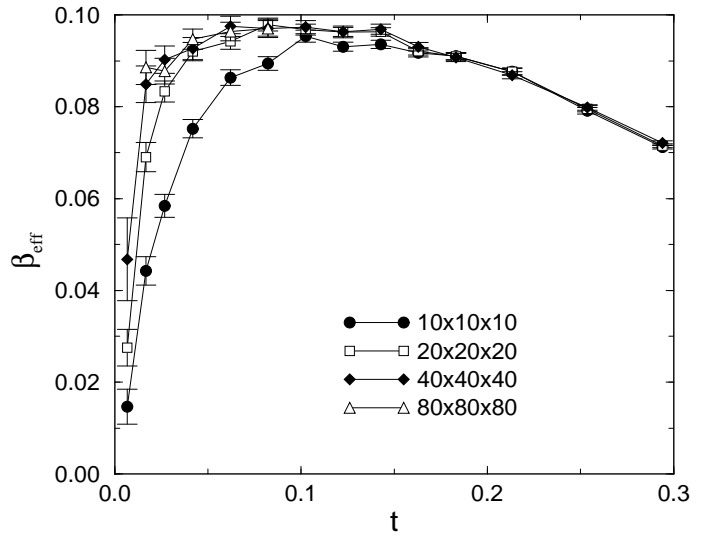


FIG. 5. Effective exponent  $\beta_{eff}$  of the edge magnetization as a function of reduced temperature  $t = |T_s - T|/T_s$  at  $J_e = J_{es} = J_s = 2J_b$  for Monte Carlo systems of various sizes.

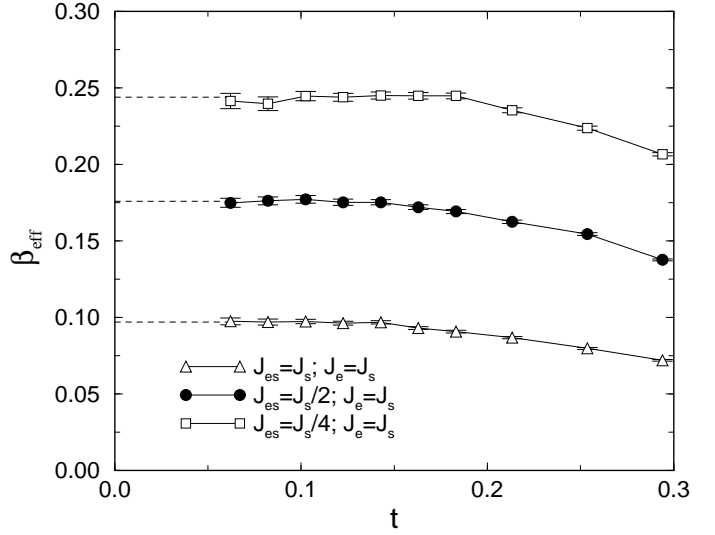


FIG. 6. Effective exponent  $\beta_{eff}$  versus reduced temperature  $t$  for different edge-surface couplings  $J_{es}$ , with  $J_e = J_s = 2J_b$ . System sizes have been adjusted to circumvent finite-size dependences, with up to  $80^3$  spins.

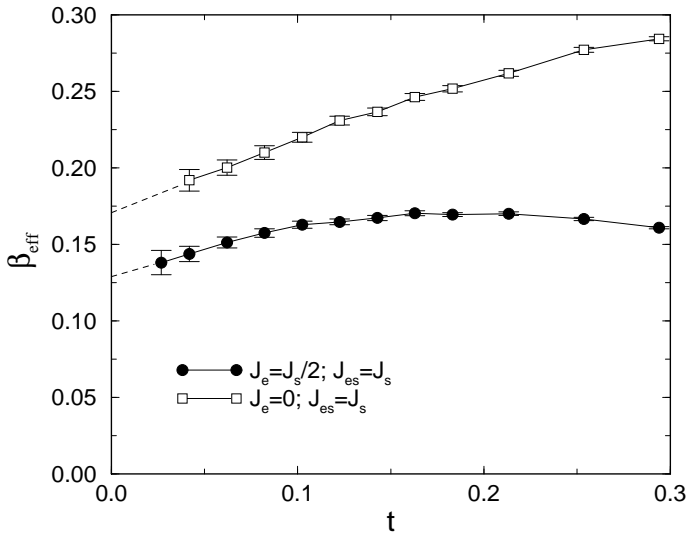


FIG. 7. Effective exponent  $\beta_{eff}$  versus reduced temperature  $t$  for different edge couplings  $J_e$ , with  $J_{es} = J_s = 2J_b$ . System sizes for the simulations have been chosen to avoid finite-size effects, with up to  $80^3$  spins close to the surface transition.